Crystal Structure of the Calcium-stabilized Human Factor IX Gla Domain Bound to a Conformation-specific Anti-factor IX Antibody

THE JOURNAL OF BIOLOGICAL CHEMISTRY
Vol. 279, No. 14, Issue of April 2, pp. 14338–14346, 2004
Printed in U.S.A.

Crystal Structure of the Calcium-stabilized Human Factor IX Gla Domain Bound to a Conformation-specific Anti-factor IX Antibody*

Received for publication, December 22, 2003
Published, JBC Papers in Press, January 13, 2004, DOI 10.1074/jbc.M314011200

Mingdong Huang, Barbara C. Furie, and Bruce Furie‡

From the Center for Hemostasis, Thrombosis and Vascular Biology, Beth Israel Deaconess Medical Center and Harvard Medical School, Boston, Massachusetts 02215

The binding of Factor IX to membranes during blood coagulation is mediated by the N-terminal γ-carboxyglutamic acid-rich (Gla) domain, a membrane-anchoring domain found on vitamin K-dependent blood coagulation and regulatory proteins. Conformation-specific anti-Factor IX antibodies are directed at the calcium-stabilized Gla domain and interfere with Factor IX-membrane interaction. One such antibody, 10C12, recognizes the calcium-stabilized form of the Gla domain of Factor IX. We prepared the fully carboxylated Gla domain of Factor IX by solid phase peptide synthesis and crystallized Factor IX-(1–47) in complex with Fab fragments of the 10C12 antibody. The overall structure of the Gla domain in the Factor IX-(1–47)-antibody complex at 2.2 Å is similar to the structure of the Factor IX Gla domain in the presence of calcium ions as determined by NMR spectroscopy (Freedman, S. J., Furie, B. C., Furie, B., and Baleja, J. D. (1995) *Biochemistry* 34, 12126–12137) and by x-ray crystallography (Shikamoto, Y., Morita, T., Fujimoto, Z., and Mizuno, H. (2003) *J. Biol. Chem.* 278, 24090–24094). The complex structure shows that the complementarity determining region loops of the 10C12 antibody form a hydrophobic pocket to accommodate the hydrophobic patch of the Gla domain consisting of Leu-6, Phe-9, and Val-10. Polar interactions also play an important role in the antibody-antigen recognition. Furthermore, the calcium coordination network of the Factor IX Gla domain is different than in Gla domain structures of other vitamin K-dependent proteins. We conclude that this antibody is directed at the membrane binding site in the ω loop of Factor IX and blocks Factor IX function by inhibiting its interaction with membranes.

Factor IX plays an important role in an intermediate stage of the blood coagulation cascade (1). Factor IX can be activated to Factor IXa in the presence of calcium ions either by Factor XIa or by the complex of Factor VIIa-tissue factor bound on membrane surfaces. Factor IXa and its cofactor, Factor VIIIa, assemble to form a membrane surface-bound enzyme complex that can efficiently activate Factor X to Factor Xa in the presence of calcium ions. Defective activity or deficiency of Factor IX due to mutation of the Factor IX gene is the cause of hemophilia B.

The vitamin K-dependent blood coagulation and regulatory proteins require vitamin K for the posttranslational synthesis of γ-carboxyglutamic acid, an amino acid clustered in the N-terminal Gla[1] domain of these proteins. The Gla domain is a membrane binding motif that, in the presence of calcium ions, supports interaction of these proteins with phospholipid membranes that include phosphatidylserine. We have recently reported the crystal structure of prothrombin fragment 1 bound to lysophosphatidylserine (2). The serine head group binds Gla domain-bound Ca-5 and Ca-6 and Gla residues 17 and 21, fixed elements of the Gla domain-fold, predicting the structural basis for phosphatidylserine specificity among Gla domains. The x-ray crystal structure of porcine Factor IX, performed in the absence of calcium, revealed the structure of the two epidermal growth factor domains and the serine protease domain but only a small C-terminal portion of the Gla domain because of disorder in the Gla domain in the absence of metal ions (3). Efforts to crystallize intact Factor IX in the presence of calcium by our group and others have been unsuccessful. NMR studies of the Factor IX Gla domain in solution indicate a largely disordered and unstructured peptide in the absence of metal ions, but this domain folds into a stable structure in the presence of calcium ions (4–6). Based upon these studies, we have demonstrated that the phospholipid binding site is located in the ω loop, the N terminus of the Gla domain. However, the positions of calcium ions and an understanding of the coordination of calcium ions by γ-carboxyglutamic acid could not be determined except by extrapolation from the known structure of the Gla domain of prothrombin (7) and by molecular modeling and energy minimization (8).

Recently, the structure of bovine Factor IX-(1–46) bound to a snake venom protein, Factor IX-binding protein, has been crystallized in the presence of calcium and magnesium ions and in the presence of calcium alone (9). Although the emphasis of this work is on the possible role of magnesium in Gla domain binding to membrane surfaces, examination of the calcium-Factor IX-(1–46) complex revealed that the calcium coordination within the Gla domain differs from the Gla domains of other vitamin K-dependent proteins, including prothrombin (7), Factor VII (10), and Factor X (11). This may be due to perturbations of the Factor IX Gla domain structure by the bound venom FIX-binding protein, or it may represent differences in the fine structure of the γ-carboxyglutamic acid-cal-

* This work was supported by grants (to B. F. and B. C. F.) from the National Institutes of Health. The costs of publication of this article were defrayed in part by the payment of page charges. This article must therefore be hereby marked "*advertisement*" in accordance with 18 U.S.C. Section 1734 solely to indicate this fact.

The atomic coordinates and structure factors (code 1NL0) have been deposited in the Protein Data Bank, Research Collaboratory for Structural Bioinformatics, Rutgers University, New Brunswick, NJ (http://www.rcsb.org/).

‡ To whom correspondence should be addressed: Beth Israel Deaconess Medical Center, 330 Brookline Ave., Boston, MA 02215.

[1] The abbreviations used are: Gla, γ-carboxyglutamic acid; FIX, Factor IX; CDR, complementarity determining region; r.m.s.d., root mean square deviation; MES, 4-morpholineethanesulfonic acid; NMP, *N*-methylpyrrolidone; L, light chain; H, heavy chain; HC, heavy chain constant domain; HV, heavy chain variable domain; LC, light chain constant domain.

cium network compared with other vitamin K-dependent proteins.

Fab fragments of antibodies have facilitated the crystallization of proteins (12). Using an anti-Factor IX antibody, 10C12, we have formed diffraction-quality single crystals of the Factor IX Gla domain-Fab 10C12 complex. Anti-Factor IX antibody 10C12 was one of a panel of antibodies identified from a phage display single-chain Fv (scFv) human antibody library screened against a synthetic Factor IX Gla domain in the presence of calcium ions (13). 10C12 was then reformatted into a $F(ab')_2$-like form with two Fab fragments connected by a leucine zipper. A conformation-specific antibody, 10C12, similar to those that bind prothrombin or Factor IX in the presence of calcium ions but not in the presence of magnesium ions (14–16) is a calcium-dependent and calcium-specific antibody for Factor IX. There was no binding in the presence of magnesium ions (17, 18).

We report here the crystal structure of the Factor IX Gla domain in the presence of calcium ions in complex with the 10C12 Fab fragment of a conformation-specific antibody directed against the calcium-stabilized form of the Gla domain of Factor IX. We identify the Factor IX-antibody interface that provides a structural basis to understanding the inhibition of membrane binding by this conformation-specific antibody. Furthermore, the marked similarity of the positions of bound calcium ions and the coordination network that defines the interaction of γ-carboxyglutamic acids with calcium ions in our Factor IX Gla domain structure, bound to the conformation-specific antibody at the hydrophobic patch (Leu-6, Phe-9, and Val-10) in the ω loop and the bovine Factor IX Gla domain bound to the venom Factor IX binding protein on a surface on the side of the Gla domain involving Phe-25, indicates that the differences observed between the Factor IX γ-carboxyglutamic acid-calcium coordination network and the Gla domains of other vitamin K-dependent proteins are not due to perturbation of the structure of the Gla domain by bound protein.

EXPERIMENTAL PROCEDURES

Materials—10C12 $F(ab')_2$ was a kind gift from Drs. C. J. Refino and D. Kirchhofer (Genentech). Protein concentration was assayed using the Advanced Protein Assay (Cytoskeleton, Denver, CO). Mecuripapain and cysteine were purchased from Sigma. Iodoacetamide was from Pierce Biotechnology (Rockford, IL). Mecuripapain (final concentration 0.5 mg/ml) was activated at 37 °C for 15 min with 10 mM cysteine in 0.1 M sodium acetate, pH 5.5, 12.5 mM EDTA.

Preparation of 10C12 Fab Fragments—The following were the optimized digestion conditions after different antibody to papain ratios, incubation time, and quenching conditions were tested. Reaction buffer (95 μl; 1.0 M sodium acetate, pH 5.5, 0.5 M NaCl) and 241 μl of activated papain (0.5 mg/ml) were added to 710 μl of 10C12 $F(ab')_2$ (1.6 mg/ml). The digestion mixture was incubated at 37 °C for 2 h, and the reaction was terminated by the addition of 120 μl of 0.1 M iodoacetamide. The reaction mixture was then applied to a HiLoad 16/60 Superdex 75 gel filtration column, and the column eluted with 0.2 M NaCl, 2 mM $CaCl_2$, 25 mM MES at pH 5.8.

Chemical Synthesis of Factor IX-(1–47)—Peptides were synthesized using Fmoc (*N*-(9-fluorenyl)methoxycarbonyl)/*N*-methylpyrrolidone (NMP) chemistry on an Applied Biosystems Model 430A peptide synthesizer. Amino acids were coupled as 1-hydroxybenzotriazole esters onto *p*-hydroxymethylphenoxymethylpolystyrene resin preloaded with aspartic acid (Applied Biosystems, Foster City, CA). All of the residues from cycle 20 through 47 were double-coupled. Following each coupling, all of the uncoupled α-N termini were acetylated. Gla residues were coupled using modified activation, coupling, and deprotection cycles. Gla (1 mmol) was dissolved in 0.4 ml of dichloromethane and 1.0 ml of *N*-hydroxybenzotriazole/NMP for 1 h with nitrogen agitation. Coupling onto a deprotected resin-bound amino acid proceeded for a total of 90 min with constant vortexing. After removal of amino acid solution and washing with NMP, Gla residues were deprotected with 20% piperidine/NMP for 30 min. Five NMP washes were done prior to the next amino acid addition.

Cleavage of the peptide from its solid support and simultaneous side chain deprotection was performed using trifluoroacetic acid/water/thioanisole/phenol/1,2-ethanedithiol (82.5:5:5:5:2.5). The cleavage reaction was allowed to proceed for 5 h at 25 °C. The peptide was then purified on a C18 high pressure liquid chromatography column eluted with an acetonitrile/water gradient. Lyophilized Factor IX-(1–47) (1.2 mg) was dissolved in 1.2 ml of sodium acetate, pH 5.5, 0.5 M NaCl. This solution was transferred to an Eppendorf tube containing 24 μl of 20 mM $CaCl_2$ and then to 12 μl of 0.2 M $CaCl_2$ to raise the final calcium chloride concentration to 2 mM. The reconstituted Factor IX-(1–47) remained clear at room temperature indefinitely but precipitated when stored at 4 °C.

10C12 Fab-Factor IX-(1–47) Complex Formation and Crystallization—10C12 Fab fragment (4 ml; 0.18 mg/ml) was mixed with 1 ml of Factor IX-(1–47) at 0.50 mg/ml. The complex was purified on a HiLoad 16/60 Superdex 75 gel filtration column to eliminate aggregates using 0.2 M NaCl, 2 mM $CaCl_2$, 0.1 M HEPES, pH 7.5. The purified protein was concentrated in a Millipore Ultrafree concentrator with 5,000 molecular weight cutoff to a concentration of 4.0 mg/ml. Crystals of 10C12 Fab-Factor IX-(1–47) complex were formed using the sitting drop vapor diffusion method at a precipitant condition of 2.3 M ammonium sulfate, 0.1 M HEPES, pH 7.5, 5 mM calcium chloride, 2% 2-methyl-2,4-pentanediol. The crystals were rapidly soaked in mother liquor containing 25% glycerol and then flash-frozen in a liquid nitrogen stream and mounted in the goniometer head for diffraction data collection.

X-ray Data Collection and Structure Determination—The x-ray diffraction data used to determine the crystal structure 10C12 Fab-Factor IX-(1–47) complex were collected at beam lines ×12c and ×25. All of the diffraction data were indexed and processed using the HKL2000 suite (19).

The structure was determined by the molecular replacement method with AMORE software (20). Homology models of 10C12 Fab heavy and light chains were built from their sequences by program SwissProt (21). The template PDB coordinates used for homology modeling were as follows: 2FB4L, 2IG2L, 1DCLB, 1DCLA, and 3MCG2 for the light chain, and 2IG2H, 1AQKH, 8FABD, 1DFBH, and 2FB4H for the heavy chain, respectively. This Fab model was then separated into four domains to be used as molecular replacement models: heavy chain constant domain (HC), heavy chain variable domain (HV), light chain constant domain (LC), and light chain variable domain. Models from domain HC, HV, and LC gave distinguishable AMORE molecular replacement rotational solutions with the height of first peaks approximately 16 higher than the strongest noise peak (defined as peak drop) at a resolution range of 8–4 Å. At the translational function step of the molecular replacement method, however, only the LC model gave discernible AMORE translation function solutions that were 1.2σ higher than the strongest noise peaks and had a correlation coefficient of 0.55 at a 15–4-Å resolution range. This LC model was then fixed and used to search for the positions of the rest of the models, yielding translation function peak drop/correlation coefficients of 3.7σ/53.0, 4.0σ/53.9, and 7.3σ/52.9 for HC, HV, and light chain variable domains, respectively. All of these domains assembled properly into a Fab molecule and packed well inside a crystal lattice without severe overlap with symmetry-related molecules. This Fab fragment was refined successfully to R and R_{free} values of 0.305 and 0.372, respectively, by CNS (22), further confirming the correct molecular replacement solution of the Fab fragment. At this stage, the correct conformations of side chains of complementarity determining regions (CDR) were clearly visible in $3F_o - 2F_c$ σ_A-weighted electron density maps (23)and were adjusted or built-in manually using the graphic program (24). Molecular replacement using models derived from other Gla domain structures failed despite the high degree of sequence and structural homology among the known Gla domains (7, 10, 11). However, the $3F_o - 2F_c$ σ_A-weighted electron density maps revealed some connected density, presumably Gla domain, next to Fab CDR loops. A Gla domain model derived from the crystal structure of the Factor X Gla domain-Factor X-binding protein complex (11) was then manually positioned into this electron density. The resulting Gla domain packed well with neighboring molecules and was successfully refined with molecular dynamic simulated annealing and conjugate gradient minimization protocols together with some manual adjustment to final R and R_{free} values of 0.233 and 0.270, respectively.

For structural analysis and graphic representation, MOLSCRIPT (25), BOBSCRIPT (26), RASTER3D (27), and GRASP (28) programs were used. Hydrogen bonds and van der Waals contacts in the final model were identified using the programs HBPLUS (29) and LIGPLOT (30).

TABLE I
Summary of X-ray diffraction data collection and model refinement for 10C12 Fab-factor IX Gla domain complex crystal

Temperature for data collection	−170 °C
Crystal diffraction limit	2.10 Å
Total number of reflections	241,036
No. of unique reflections	28,585 (1353)[c]
Overall data redundancy	8.4
Data completeness	81.9% (38.7%)[c]
Data R_{merge}[a]	0.050 (0.119)[c]
Data I/σ	25.7 (5.4)[c]
Model refinement	
Protein/solvent atoms	3640/148
Calcium/sulfate ions	6/1
Resolution for refinement	24.66–2.20
R_{cryst}[b] values	0.233 (0.278)[c]
R_{free} value	0.270 (0.332)[c] for 1298 reflection (4.9%)
Estimated coordinate error	0.31 Å (from Luzatti plot (47))
R.m.s.d. for bond lengths	0.006 Å
R.m.s.d. for bond angles	1.7°
Ramachandran plot from program PROCHECK (48)	88.0% most favored; 11.1% allowed; 0.5% generally allowed; 0% disallowed

[a] $R_{merge} = \Sigma_h\Sigma_i|I_i(h) - (I(h))|/\Sigma_h\Sigma_i I_i(h)$, where $(I(h))$ is the mean intensity, $I(h)$, of reflection h.
[b] $R_{cryst} = \Sigma_{hkl}|F_o - F_c|/\Sigma_{hkl} F_o$.
[c] Numbers in parentheses refer to the highest resolution shell.

RESULTS

Structure of 10C12 Fab-Factor IX-(1–47) Complex—The structure of 10C12 Fab-Factor IX-(1–47) complex was determined by x-ray crystallography to 2.2 Å. The coordinates of this complex have been deposited as 1NL0 in the Protein Data bank. The current model consists of residues 1–210 of the 10C12 light chain, residues 1–126 and 135–217 of the 10C12 heavy chain, residues 1–45 of the Factor IX-(1–47), and 148 loosely attached solvent molecules (Table I). The model was refined at 2.2 Å to R_{cryst} and R_{free} values of 0.233 and 0.270, respectively (Table I). Most of the bond angles of residues are clustered in energetically favorable (88.0%) or allowed (11.1%) regions of the Ramachandran plot. Residue Asp-152L of the 10C12 Fab fragment was clearly defined by the electron density maps but located outside of these regions. This is probably because this side chain makes hydrogen bonds to the imidazole ring of His-189L and the main chain N atom of Lys-190L partially compensating for the high energy conformation (Φ/Ψ = 69.8°/−97.0°) of its main chain. Residue 51L of 10C12 also adopts a high energy conformation (Φ/Ψ = 68.1°/−45.1°), a situation commonly found in antibody structures (for example, see Ref. 31). Disorder around the heavy chain residues near residue 130 is also often observed in antibody structures. Residues 127–134 of the 10C12 heavy chain were not included in the current model because of poorly defined electron density in this region. Two C-terminal residues of the Factor IX-(1–47), residues 46 and 47, did not have well defined electron densities and were omitted from the final model.

The crystal structure of the complex of the 10C12 Fab and Factor IX-(1–47) indicates the interaction of the antibody with the N-terminal ω loop of Factor IX (Fig. 1). Fab 10C12 is typical of an anti-protein antibody with six CDR loops forming a concave and undulating antigen binding surface (32). CDR loops H1, H2, H3, and L3 from this antigen binding surface form a hydrophobic pocket that binds exposed N-terminal residues of Factor IX-(1–47), resulting in an interface with a total area of 1338 Å^2. This interface is one of the smallest among protein-anti-protein antibody complexes (29) despite the high affinity interaction (K_d 1.6 nM) between 10C12 Fab and Factor IX-(1–47) (13). Although 10C12 is a calcium-dependent conformation-specific antibody recognizing only the calcium-stabilized Factor IX-(1–47) conformer, no direct interactions between the Fab fragment of the antibody and calcium ions in the Gla domain were observed.

10C12 Fab-Factor IX Gla Interactions—Despite sequence similarities within the N terminus of the vitamin K-dependent proteins (Fig. 2), the 10C12 antibody is specific for Factor IX and does not bind to the Gla domains of other vitamin K-dependent proteins, although it does bind to Factor IX of other species. A hydrophobic pocket is formed from 10C12 Fab CDR heavy chain residues Ala-33, His-35, Ile-50, Tyr-52A, Ser-52, Lys-56, Tyr-58, Ala-98, Ala-100, Arg-100A, and CDR light chain residues Trp-91 and Phe-96 (Fig. 3) (numbered using the Kabat-Wu system (33)). Light chain residue Phe-96 and heavy chain residues Ile-50 and His-35 constitute the bottom of the pocket. The wall of the pocket is built in part by heavy chain residues Tyr-58, Lys-56, and Ser-52 and in part by light chain residue Trp-91. Heavy chain residue Ala-100 defines a protrusion in wall of the hydrophobic pocket. The presence of glycine

FIG. 1. **Crystal structure of the complex of the 10C12 Fab and Factor IX-(1–47).** A ribbon diagram depicts the Fab fragment of the antibody 10C12. Light chain is shown in *light blue*, and heavy chain is shown in *dark blue*. Factor IX-(1–47) is also shown as a ribbon diagram, *colored blue* to *yellow* from the N terminus to the C terminus. Six calcium ions are shown from Ca-1 to Ca-7. Ca-6 is not present in this structure. Residues 1, 5, 6, 9, 11, and 45 in Factor IX-(1–47) are labeled. The side chains of residues 5, 6, 9, and 11 are included.

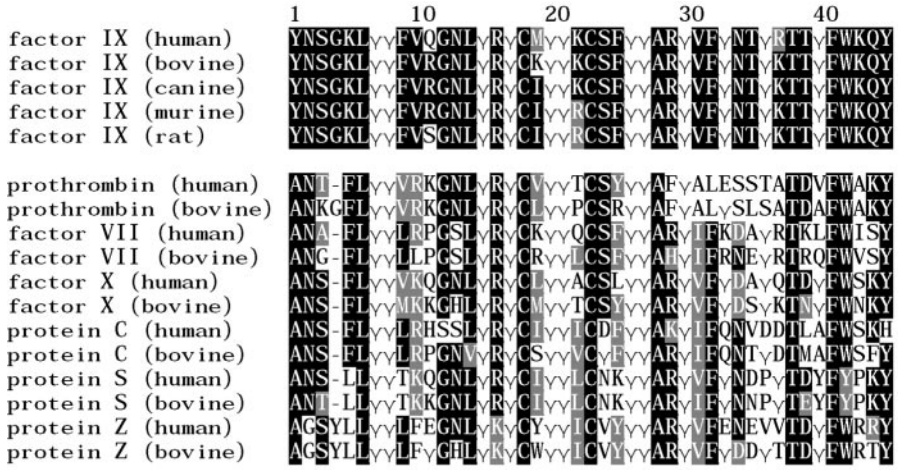

FIG. 2. **Alignment of N-terminal amino acid sequences of vitamin K-dependent proteins.** γ, γ-carboxyglutamic acid, is not highlighted. Relative to the consensus sequence in each group, residues in Factor IX and the vitamin K-dependent proteins are coded as *black* (identity), *gray* (conserved), or *white*.

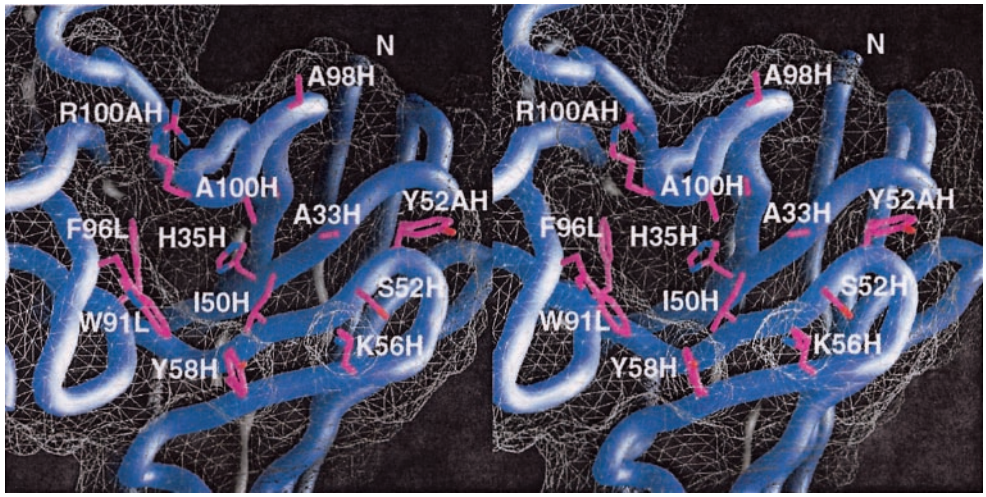

FIG. 3. **The CDR loops of 10C12 Fab form a hydrophobic pocket.** The CDR loops of 10C12 Fab (*blue tubes*) form a hydrophobic pocket as shown as a stereoimage. The molecular surface of 10C12 Fab is represented by the *white net*. The carbon atoms of 10C12 Fab CDR residues that form the hydrophobic pocket are *colored* in *magenta*.

instead of alanine at this residue greatly reduced the affinity between this antibody and the Factor IX Gla domain (13), illustrating the importance of the shape of this pocket. The hydrophobic pocket accommodates the antigenic determinant within Factor IX, including Lys-5, Leu-6, Phe-9, Val-10, and Gln-11. Polar interactions are limited to the electrostatic interaction between Lys-5 on Factor IX and Asp-93 and Asn-31 on the antibody light chain. Only four hydrogen bonds were found between 10C12 and Factor IX-(1–47) (Table II).

A representative electron density map of one region of the antibody-antigen interface is shown in Fig. 4. The conformations of most of the residues are well defined by the electron density map. This map illustrates a unique conformation of the 10C12 CDR3 loop of the heavy chain (residues 96H–100H), a tight β turn characterized by a hydrogen bond between side chains in addition to the usual main chain hydrogen bond between i and i+3 residues.

Gln-11 of Factor IX-(1–47) interacts with all three CDR loops of the Fab heavy chain. The amide nitrogen atom of Gln-11 forms a hydrogen bond (2.49 Å) to the 10C12 heavy chain residue Thr-31. Water molecules also mediate the interaction between Factor IX and the antibody. A cavity identified in the antibody-antigen interface is occupied by a water molecule (S148).

Structure of the Factor IX-(1–47)—The Gla domain of Factor IX consists of an N-terminal ω loop and three short α-helixes (helix A: residues 14–19; helix B: residues 24–32; helix C: residues 35–45) (Figs. 5 and 7). Most of the calcium ions (numbered 1–5) are positioned between the ω loop and the A and B helices with calcium liganding providing the folding energy to align the ω loop properly. Helices A and B are connected by a tight turn and further stabilized by a conserved disulfide bond between residues 18 and 23 of the Gla domain. The two cysteine residues also form two hydrogen bonds (Tyr-45 to Cys-18, 3.10 Å; Tyr-45 to Cys-23, 2.88 Å) to the side chain of a conserved Tyr-45 of helix C, providing an anchor to bundle three helices together. This tyrosine residue and the disulfide bond are part of the hydrophobic core between helix C and helix A/B that includes Phe-25, Ala-28, Phe-41, and Trp-42, a cluster that provides further hydrophobic energy to bind helix C to helix A/B. All of these residues are conserved among Gla domains of vitamin K-dependent proteins.

Calcium Ions in the Factor IX Gla Domain—Calcium ions are required for the folding of Gla domains into functional membrane binding structures. In our Factor IX-(1–47) structure, a total of six calcium ions were observed. γ-Carboxyglutamic acid plays a critical role in the coordination of calcium ions in Factor IX as it does in the other known vitamin K-dependent blood coagulation and regulatory proteins. Ca-4 is unique in that it is held in place by carboxyl groups contributed by four γ-carboxyglutamic acid residues. The calcium ion coordination for Factor IX-(1–47)-10C12 Fab is shown in Table III. Five calcium ions (Ca-1 to Ca-5) are aligned (3.7–4.0-Å spacing) at the core of the Gla domain

TABLE II
Interactions of specific atoms in Factor IX-(1–47) and 10C12 Fab

Factor IX-(1–47)	10C12	Distance
		Å
Hydrogen bonds		
Phe-9 (O)	Tyr-52AH (N)	2.98
Gln-11 (NE2)	Thr-31H (OG1)	2.49
Lys-5 (NZ)	Asp-93L (OD1)	2.81
Lys-5 (NZ)	Asn-31L (OD1)	2.74
van der Waals contacts		
Leu-6 (CB)	Ala-100H (CB)	3.68
Leu-6 (CD1)	Trp-91L (CZ3)	3.76
Leu-6 (CD1)	Trp-91L (CE3)	3.47
Leu-6 (CD2)	Trp-91L (CH2)	3.50
Leu-6 (CD2)	Trp-91L (CZ3)	3.56
Leu-6 (CD2)	Tyr-58H (CE2)	3.39
Leu-6 (CD2)	Tyr-58H (CD2)	3.38
Leu-6 (CG)	Trp-91L (CZ3)	3.82
Leu-6 (CG)	Trp-91L (CE3)	3.74
Leu-6 (CG)	Trp-91L (CD2)	3.89
Gla-8 (C)	Lys-56H (CD)	3.84
Phe-9 (CA)	Ser-52H (CB)	3.73
Phe-9 (CB)	Ser-52H (CA)	3.88
Phe-9 (CD2)	Ser-52H (CB)	3.89
Phe-9 (CD2)	Ser-52H (CA)	3.64
Phe-9 (CD2)	Ile-51H (C)	3.76
Phe-9 (CD2)	Ile-50H (CG1)	3.74
Phe-9 (CE1)	Tyr-58H (CZ)	3.59
Phe-9 (CE1)	Tyr-58H (CE2)	3.20
Phe-9 (CE1)	Tyr-58H (CD2)	3.69
Phe-9 (CE1)	Lys-56H (CD)	3.84
Phe-9 (CE2)	Lys-57H (CA)	3.42
Phe-9 (CE2)	Lys-56H (C)	3.41
Phe-9 (CE2)	Lys-56H (CG)	3.88
Phe-9 (CE2)	Lys-56H (CB)	3.84
Phe-9 (CZ)	Tyr-58H (CZ)	3.68
Phe-9 (CZ)	Tyr-58H (CE2)	3.40
Phe-9 (CZ)	Tyr-58H (CD2)	3.45
Phe-9 (CZ)	Tyr-58H (CG)	3.80
Phe-9 (CZ)	Lys-56H (CB)	3.87
Val-10 (C)	Tyr-52AH (CD1)	3.70
Val-10 (CG1)	Ala-98H (CA)	3.85
Gln-11 (CA)	Tyr-52AH (CZ)	3.87
Gln-11 (CA)	Tyr-52AH (CE1)	3.60
Gln-11 (CA)	Tyr-52AH (CD1)	3.67

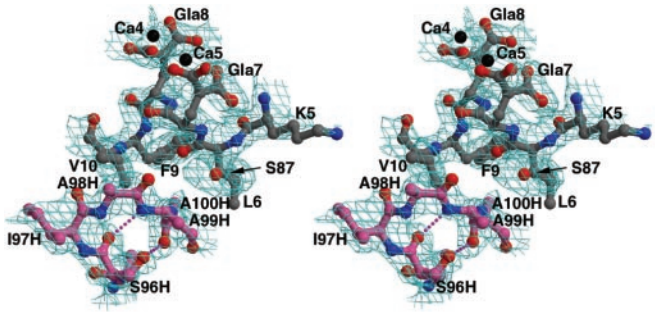

FIG. 4. **Electron density map of the CDR3 loop of the heavy chain of 10C12 Fab and the ω loop of Factor IX-(1–47).** The representative electron density net is shown in *cyan*. The Factor IX Gla domain ω loop is shown with carbon atoms in *gray*. The 10C12 Fab CDR H3 loop is shown with carbon atoms in *magenta*. The 10C12 H3 loop forms a tight β-turn stabilized by two hydrogen bonds (*red dashed line*). For clarity, the electron density associated with Ca-4 and Ca-5 has been deleted.

coordinated by carboxyl groups of Gla residues (Fig. 6). This calcium array is distant (~13 Å) from the antibody-combining site. The positions of each of these calcium ions are nearly identical to that in bovine Factor IX-(1–46) in the Factor IX-(1–46)-Factor IX-binding protein complex (r.m.s.d. 0.203 Å) (9). Ca-6, which is observed in other Gla domains including bovine Factor IX-(1–46) in the Factor IX-(1–46)-Factor IX-binding protein complex, was not detected in our Factor IX-(1–47) structure, presumably because of the high concentration of ammonium sulfate used during crystallization of Factor IX-(1–47)-10C12 Fab.

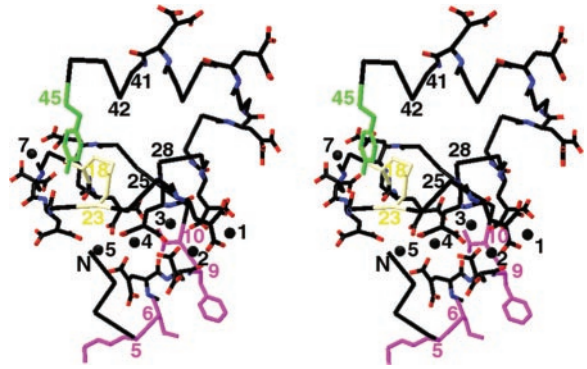

FIG. 5. **Gla domain of Factor IX.** The Gla domain structure shown as a stereoimage includes calcium ions 1, 2, 3, 4, 5, and 7 as *black spheres*), residues 5, 6, 9, and 10 in *magenta*, cysteines 18 and 23 in *yellow*, tyrosine 45 in *green*, Gla residue side chains and peptide backbone in Corey-Pauling-K. Hung *coloring*.

Gla-36 and Gla-40 are unique to Factor IX and the analogous residues in Factor X. In the Factor X Gla domain structure (11) and the Factor IX-(1–46)-Factor IX-binding protein complex (9), a calcium ion was located between the side chains of these two Gla residues that are adjacent in the three-dimensional structure. In our Factor IX-(1–47) structure, these two Gla residue side chains adopt similar conformations as in Factor X and Factor IX-(1–46), although the electron density for the side chain of Gla-36 was weak and not well defined. However, the electron density maps and molecular dynamic refinement suggest that a similar calcium ion does not exist in our Factor IX-(1–47). Given crystallization conditions using high concentrations of ammonium sulfate, we suspect that this is a weak calcium binding site that is not occupied by calcium under the conditions employed. The carboxylation at these two positions were not required for Factor IX function in Factor X activation and coagulant activity (34).

Stability of the ω Loop: Comparison of the Structure of Human Factor IX-(1–47) from X-ray Crystallography with the Solution Structure of Factor IX-(1–47) Determined by NMR Spectroscopy and with the X-ray Crystallographic Structures of Gla Domains of Other Vitamin K-dependent Blood Coagulation Proteins—Our Factor IX-(1–47)-10C12 Fab structure indicates that the 10C12 antibody directly binds to the Factor IX ω loop, the structural determinant important for Gla domain cell surface anchoring. The bound 10C12 antibody does not appear to perturb the structure of Factor IX-(1–47), specifically at the antibody combining site interface with the Factor IX ω loop. Structural comparison of our human Factor IX-(1–47) in the Factor IX-(1–47)-10C12 complex and the bovine Factor IX in the Factor IX-(1–46)-IX binding protein complex suggests that the Factor IX structures are very similar (r.m.s.d. of 0.465 Å for 44 Cα atoms), although each Factor IX has the potential of being structurally perturbed by another bound protein (Fig. 1) (see Fig. 4*C* of Ref. 9). The structural similarity of our Factor IX-(1–47) to other Gla domains is also significant (Fig. 7). The r.m.s.d. of the Cα atoms between Factor IX-(1–47) and the prothrombin, Factor X, and Factor VII Gla domains are 0.89, 0.63, and 0.63 Å, respectively. These results suggest that the ω loop of Factor IX-(1–47) is quite stable and the 10C12 Fab binding does not induce significant structural change.

Comparing other Gla domain structures, our Factor IX-(1–47) shows significant differences in the fine structure, specifically the positions and role of certain amino acid side chains. For example, variations among crystal structures of Gla do-

TABLE III
Comparison of the calcium ion coordinations for Factor IX-(1–47)

	NMR-derived Factor IX structure (5)	Molecular Dynamics- derived Factor IX structure (8)	X-ray-derived Factor IX structure (This work)	X-ray-derived Factor IX structure (9)
Ca-1	Gla-26-OE1 Gla-26-OE4	Gla-26-OE1 Gla-26-OE4	Gla-26-OE1 Gla-26-OE4 Gla-30-OE1 Gla-30-OE4 H_2O 159	Gla-26-OE2 (eq.to OE1) Gla-26-OE3 (eq. to OE4) Gla-30-OE2 (eq. to OE1) Gla-30-OE4
Ca-2	Gla-8-OE2 Gla-30-OE3 Gla-30-OE4	Gla-8-OE2 Gla-30-OE3 Gla-8-OE4 Gla-30-OE2	Gla-8-OE2 Gla-30-OE3 Gla-30-OE4 Gla-8-OE3 (eq. to OE4) Gla-27-OE1 H_2O 159	Gla-8-OE1 (eq. to OE2) Gla-30-OE3 Gla-30-OE4 Gla-8-OE4 Gla-27-OE1
Ca-3	Gla-7-OE3 Gla-8-OE1 Gla-27-OE2	Gla-7-OE3 Gla-8-OE1 Gla-27-OE2 Asn-2-OD1 Gla-8-OE2 Gla-27-OE1 Gla-30-OE3 Gla-30-OE4	Gla-27-OE2 Gla-30-OE3 Gla-8-OE4 Gla-8-OE3 Gla-17-OE1 H_2O 110	Gla-27-OE2 Gla-30-OE3 Gla-8-OE2 (eq. to OE4) Gla-8-OE1 (eq. to OE3) Gla-17-OE4 (eq. to OE1)
Ca-4	Gla-27-OE1 Gla-27-OE4 Gla-17-OE4	Gla-27-OE1 Gla-27-OE4 Gla-7-OE3 Gla-7-OE4 Gla-17-OE2 Gla-17-OE3	Gla-27-OE2 (eq. to OE1) Gla-27-OE4 Gla-17-OE1 (eq. to OE2) Gla-17-OE3 Gla-7-OE3 Gla-8-OE4 Asn-2-OD1	Gla-27-OE2 Gla-27-OE4 Gla-17-OE2 Gla-17-OE4 (eq. to OE3) Gla-7-OE3 Gla-8-OE1 (eq. to OE4) Asn-2-OD1
Ca-5	Gla-7-OE4 Gla-17-OE2 Tyr-1-O	Tyr-1-O Ser-3-OG Gla-7-OE1 Gla-7-OE4 Gla-17-OE3	Tyr-1-O Gla-7-OE1 Gla-17-OE3 Gla-17-OE4 Gla-7-OE2 Gla-21-OE3 H_2O 79	Tyr-1-O Gla-7-OE3 (eq. to OE1) Gla-17-OE1 (eq. to OE3) Gla-17-OE2 (eq. to OE4) Gla-7-OE4 (eq. to OE2) Gla-21-OE4 (eq. to OE3)
Ca-6	Gla-21-OE1 Gla-21-OE4	Gla-21-OE1		Gla-21-OE2 (eq. to OE1) Gla-21-OE3 (eq. to OE4)
Ca-7	Gla-15-OE2 Gla-20-OE1 Gla-20-OE3	Gla-15-OE2 Gla-20-OE1 Gla-20-OE3 Gla-15-OE4	Gla-15-OE2 Gla-20-OE1 Gla-20-OE4 (eq. to OE3) Gla-15-OE4	Gla-15-OE1(eq. to OE2) Gla-20-OE3 Gla-15-OE4
Ca-8		Gla-30-OE1 Gla-30-OE2 Gla-33-OE3 Gla-33-OE4		Gla-40-OE2 Gla-40-OE4 Gla-36-OE2 Gla-36-OE3
Ca-9		Gla-36-OE4 Gla-40-OE3 Gla-36-OE1 Gla-40-OE1		

mains were seen in the ω loop region (31), perhaps corresponding to sequence variability in this region (Fig. 2). Some differences in the orientation of the side chains are also significant. Factor VII and Factor X Gla domains have a Gla residue, Gla-6, that bridges Ca-4 and Ca-5 with both carboxylate groups of its side chain (Fig. 8). This Gla residue, along with three other ω loop residues (residues 3–5), participates in a tight β-turn. In Factor IX-(1–47), the side chain of this Gla residue (Gla-7 in Factor IX numbering) rotates along its Cα-Cβ bond by ~120°. Only one carboxylate group of its side chain bridges calcium ions 4 and 5. The other carboxylate group forms hydrogen bonds to the backbone nitrogen atoms at residues 3, 4, and 5. As a result, Ca-4 has one less oxygen ligand compared with the Factor VII and Factor X Gla domains. This rotation of the Gla-7 side chain stabilizes the ω loop into a unique conformation with all of the backbone nitrogen atoms in this region oriented toward the negatively charged Gla-7. This rotation of the Gla-7 side chain is not an artifact due to the antibody 10C12 binding nor is it unique to Factor IX. Bovine prothrombin fragment 1, which is similar to Factor IX in the insertion of a glycine in its N-terminal sequence (Fig. 2), also shows a Gla-7 conformation similar to that in Factor IX. Unlike Fac-

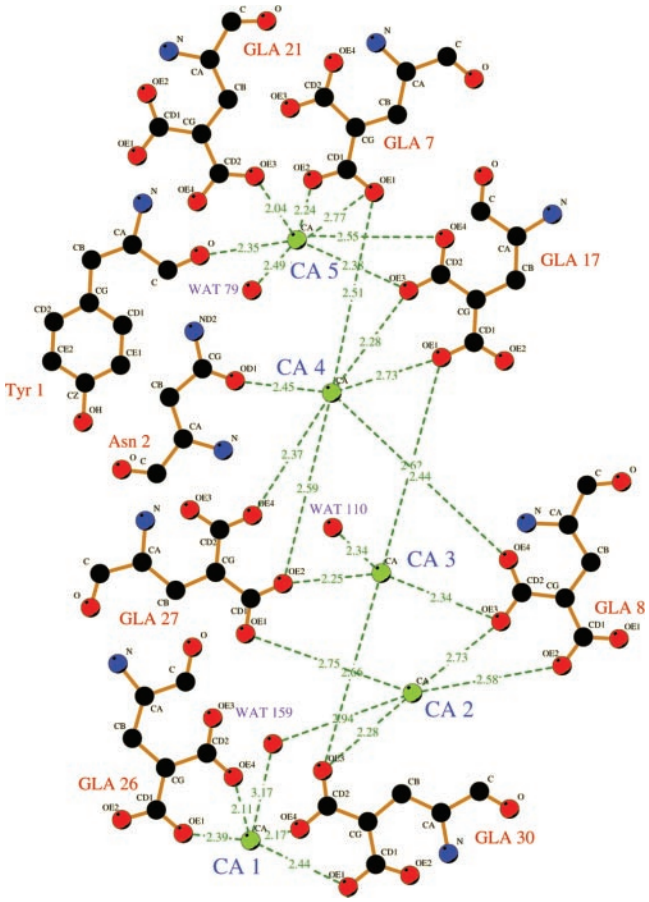

FIG. 6. **Core calcium-ligand network in the Factor IX-(1–47)-calcium complex.** The interatomic distances between oxygen ligands and calcium are shown as *green dotted lines* labeled with the distance in angstroms. The coordination of Ca-7, not located in the core calcium network, is not shown. The position of Ca-6 was not occupied in this crystal. Calcium ions (*green*); carbon (*black*); oxygen (*red*); nitrogen (*blue*).

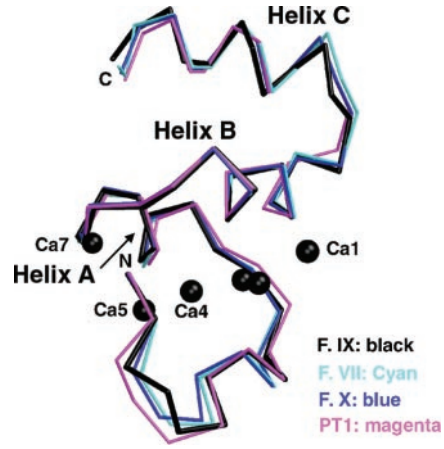

FIG. 7. **Comparison of the Gla domain polypeptide backbones.** Comparison of the polypeptide backbone of Factor IX-(1–47) with Factor X, Factor VII and prothrombin determined by x-ray crystallography. Cα trace superposition of Gla domain crystal structures of Factor IX (*black*), Factor VII (*cyan*), Factor X (*blue*), and prothrombin (*magenta*) are shown. Calcium ions are *black spheres*. Ca-6 is not occupied in our Factor IX Gla domain but is present in the bovine Factor IX-(1–46) (9) and other Gla structures in vitamin K-dependent proteins. The location of other calcium ions are highly conserved among all of the Gla structures.

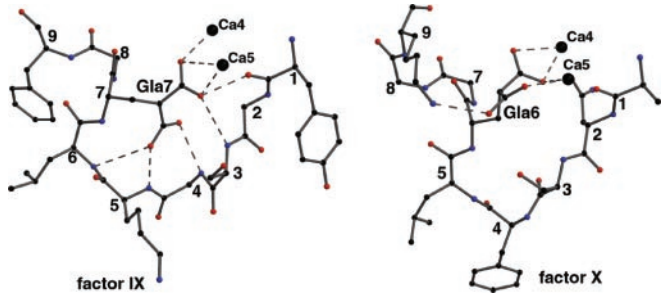

FIG. 8. **Differences of conformation of Gla-7 residues in Factor IX (*left panel*) and Factor X (*right panel*).** In Factor IX, Gla-7 stabilizes the ω loop conformation by a network of hydrogen bonds. Side chains of residue Gla-8 (in Factor IX) and Gla-7 (in Factor X) are omitted for clarity.

tor IX, bovine prothrombin fragment I adopts two conformations in its ω loop (2).

DISCUSSION

Conformation-specific antibodies directed at calcium-stabilized structures of the vitamin K-dependent proteins have been useful probes of protein structure. They have identified regions that undergo ligand-induced conformational transitions (35–37), served as solid phase immunoaffinity reagents that offer facile release of the antibody-protein complex by the addition of EDTA (14, 38), and provided novel inhibitors of protein-membrane interaction (15, 16). As an approach to developing an antibody-based therapeutic anti-thrombotic agent, the calcium-specific anti-Factor IX antibody, 10C12, was one of a panel of antibodies identified from a human single-chain variable domain antibody (scFv) library screened for binding to human Factor IX in the presence of calcium ions (13). The 10C12 scFv antibody was then reformatted into a $F(ab')_2$ where two Fab fragments were linked by a leucine zipper. The 10C12 antibody binds tightly to full-length Factor IX or activated Factor IX with a K_d of 1.6 nM and is specific for Factor IX but does not bind to the other vitamin K-dependent proteins despite the sequence similarity between the Gla domains of these proteins. The $F(ab')_2$ of 10C12 was functionally active and prolonged the partial thromboplastin time, inhibited platelet-mediated blood coagulation, and inhibited Factor X activation by Factor IXa in complex with Factor VIIIa. *In vivo*, $F(ab')_2$ 10C12 is an effective anticoagulant in several animal models (17, 18). Our Factor IX-(1–47)-10C12 crystal structure shows that the anticoagulant effect of 10C12 is due to binding to the Factor IX hydrophobic patch, a major structural determinant in the vitamin K-dependent blood coagulation proteins that participates in protein-membrane interaction (4, 39, 40).

Calcium Ion Coordination—We have identified six bound calcium ions in the Factor IX Gla domain of the human Factor IX-(1–47)-10C12 antibody complex. We used high concentrations of ammonium sulfate during crystallization of this complex and thus observed occupancy in only the higher affinity calcium binding sites. In contrast, Shikamoto *et al.* (9) observed eight calcium ions in their crystal structure of bovine Factor IX-(1–46) in the Factor IX-(1–46)-FIX-binding protein complex. These crystals were prepared in Tris-HCl, pH 8.0, 14% polyethylene glycol, and 5 mM $CaCl_2$, a system in which the free calcium ion concentration would be much higher than in ammonium sulfate. However, our recent efforts to crystal the human Factor IX-(1–47)-10C12 antibody complex using polyethylene glycol were unsuccessful. We believe that the lower affinity sites, including Ca-6 and Ca-8, were not occupied by calcium ions under our crystallization conditions because of the reduced free calcium concentration. The suggestion that Ca-6 is a low affinity site is significant because we have shown that the serine head group of lysophosphatidylserine displaces water from the coordination sphere of Ca-6 (2). The ternary complex of Ca-6, phosphatidylserine, and Factor IX may be character-

ized by tighter binding of calcium than this complex in the absence of phosphatidylserine. Ca-8, coordinated by Gla-36 and Gla-40, has no apparent functional role because elimination of these γ-carboxyglutamic acid residues does not alter the biological assays tested (34).

The positions of the six common calcium ions bound to the Factor IX Gla domain in both our human Factor-(1–47)-10C12 complex and in the bovine Factor-(1–46)-FIX-binding protein complex are nearly identical (9). Comparison of the positions of these calciums, including Ca-1 to Ca-5 and Ca-7, revealed a r.m.s.d. of 0.203 Å compared with the overall r.m.s.d. of 0.467 Å for 44 Gla domain Cα atoms. Furthermore, the coordination of these calcium ions in these two independent structures is nearly identical (Table III). Of 31 oxygen ligands to 6 calcium ions, all are identical in both structures with the exception of one. These results emphasize that the specific γ-carboxyglutamic acid-calcium network in Factor IX differs from other Gla domains.

Nine calcium ions were modeled into our NMR-derived Factor IX-(1–47)-calcium complex structure (5) as refined by molecular dynamics simulation with initial calcium positions determined by a genetic algorithm (8). Comparison of the calcium coordination of Factor IX-(1–47)-calcium from x-ray crystallography with models of Factor IX-calcium in solution derived by extension of the prothrombin structure or molecular dynamics approaches revealed some excellent predictions and several examples where modeling proved less successful. For example, the coordination of Ca-4 by carboxyl groups from Gla-27, Gla-7, and Gla-17 was predicted in the molecular dynamic analysis (Table III). The role of the carboxyl groups of Gla-17 and the hydroxyl O of Tyr-1 in coordinating Ca-5 was correctly predicted, but a role for the Gla-21 carboxyl was missed. Furthermore, a Gla-7 carboxyl group was proposed as a ligand but this was not observed in the crystal structure. These observations emphasize that the prothrombin calcium coordination, albeit similar, is not an adequate model for the Factor IX-calcium complex. In addition, molecular dynamic approaches can generate low energy models but the fine structure predicted is only a first approximation of the calcium coordination network present in Factor IX determined experimentally.

Fine Structure of the ω Loop—Although the polypeptide backbone of the ω loop in the Gla domain of the vitamin K-dependent proteins demonstrates marked structural similarity, the amino acid sequences in these regions exhibit both similarity and some critical differences. It would appear that the fine structure of the ω loop is defined by interaction of these critical side chains. We have demonstrated the special role of Gla-7 in Factor IX in orienting the polypeptide backbone and stabilizing the positions of the amide nitrogens by hydrogen bonding. This function is quite different from the homologous γ-carboxyglutamic acid residue in Factor X. We suspect that these structural differences play critical functional roles in the assembly of these proteins on membrane surfaces and during protein complex formation during blood coagulation. These structural differences appear significant and are not induced by the bound antibody because the bovine Factor-(1–46)-FIX-binding protein complex shares a similar structure.

Factor IX Specificity of 10C12 Antibody—Despite the sequence similarity, 10C12 antibody recognizes only Factor IX-(1–47) but not the Gla domains of other coagulation proteins. The Factor IX-(1–47)-10C12 structure provides a structural basis for this specificity. Table II shows all of the hydrogen bonds and van der Waals interactions between the Factor IX-(1–47) and 10C12 Fab. Of four hydrogen bonds, the Lys-5 side chain of the Gla domain forms two hydrogen bonds to the light chain of 10C12 Fab. One of the hydrogen bonds is between oppositely charged Lys-5 of the Gla domain and Asp-93L of the 10C12 Fab. This interaction is stronger than a normal hydrogen bond (4.5 *versus* 2–3 kcal/mol). Lys-5 is unique to Factor IX. All of the other Gla domain sequences have a hydrophobic residue at the corresponding position (Fig. 2). Thus, this lysine residue constitutes a major structural determinant targeted by 10C12 Fab. Hydrophobic interactions play an important role in Factor IX Gla domain-10C12 antibody binding and contribute to antibody specificity. CDR loops of 10C12 antibody form a hydrophobic pocket to accommodate the hydrophobic residues Leu-6, Phe-9, and Val-10. Although Leu-6 is conserved among Gla domains, a bulky hydrophobic residue at position 9 is unique to Factor IX.

Structural Basis of Hemophilia B Mutations in the Factor IX Gla Domain—The crystal structure of the Factor IX-(1–47) provides a framework to analyze the structural and functional consequences of naturally occurring genetic alterations in patients with hemophilia B, particularly those involving the ω loop. Naturally occurring point mutations of the Factor IX Gla domain in which the normal amino acid is substituted by another amino acid are known to occur at residues 2–9, 12, 17, 18, 20, 21, 23, 25–27, 29, 32, 33, 38, 41, 43, 45, and 46 (Ref. 41 and www.kcl.ac.uk/ip/petergreen/fix2.html), and the structure of the Gla domain of Factor IX will facilitate the understanding of structure-function relationships.

A hemophilia mutation at residue 2 (Asn → Ile) reduces circulating Factor IX antigen level to ~60% but lowers the functional activity of the mutant Factor IX to 1% of that in wild type Factor IX (42). Our Factor IX Gla structure indicates that Asn-2 is a structurally important residue. Its side chain forms hydrogen bonds to Gla-8 and Gla-27 and is a ligand for Ca-4. As the N terminus anchors one end of ω loop, the mutation of this residue will lead to destabilization of the ω loop.

Plasma from a naturally occurring hemophilia B mutant, lysine 5 → glutamate, has normal antigen levels but low Factor IX activity (43). Our Factor IX-(1–47) structure shows that Lys-5 is a surface-exposed residue and its side chain does not have a structural role in stabilizing the Gla domain. We speculate that this side chain participates in binding the phosphate group of phosphatidylserine in a manner analogous to the role of Lys-3 in prothrombin (2). Based upon the *in vivo* endothelial binding characteristics of recombinant forms of Factor IX mutated at residue 5, Gui *et al.* (44) have suggested that this residue is important for binding to collagen IV.

Gla-7 coordinates both the backbone of the ω loop and calcium 4 and 5. Naturally occurring mutations at this position greatly reduce activity, presumably by disrupting the integrity of this region.

Implication for the Mechanisms of Gla Domain Anchoring on Cell Surfaces—The Gla domains of vitamin K-dependent proteins mediate the binding of blood coagulation proteins to membrane surfaces. The Gla domains in these coagulation proteins share a high degree of sequence similarity, but their binding affinity for membrane surfaces vary over three orders of magnitude with dissociation constants ranging from nanomolar to micromolar (45). The presence of phosphatidylserine in the membrane is necessary for maximal Gla domain binding to phospholipid vesicles. Gla domains in the absence of calcium ions are largely disordered (3, 6, 39, 46). Calcium ions induce conformational changes in the Gla domain and are necessary for the Gla domain to fold properly. A common structural feature of functional Gla domains is the clustering of N-terminal hydrophobic residues into a hydrophobic patch and the exposure of this hydrophobic patch to solvent. Although this hydrophobic patch mediates Gla domain interaction with the

cell surface membrane and represents a major component of the phospholipid binding site, the specificity for phosphatidylserine is defined by electrostatic interactions between the phosphoserine head group and arginine and lysine residues in the Gla domain of prothrombin. We suspect that Lys-5 in Factor IX plays a role analogous to Lys-3 in prothrombin where, along with Arg-10, the positively charged amino acids bind to the glycerol phosphate backbone and the carboxyl group of the serine interacts with Ca-5 and Ca-6 (2).

Acknowledgments—We utilized the National Synchrotron Light Source, Brookhaven National Laboratories for beam lines ×25 and ×12c. We also thank Dr. S. J. Freedman for critical review of the paper and M. Jacobs for peptide synthesis.

REFERENCES

1. Furie, B., and Furie, B. C. (1988) *Cell* **53,** 505–518
2. Huang, M., Rigby, A. C., Morelli, X., Grant, M. A., Huang, G., Furie, B., Seaton, B., and Furie, B. C. (2003) *Nat. Struct. Biol.* **10,** 751–756
3. Brandstetter, H., Bauer, M., Huber, R., Lollar, P., and Bode, W. (1995) *Proc. Natl. Acad. Sci. U. S. A.* **92,** 9796–9800
4. Freedman, S. J., Blostein, M. D., Baleja, J. D., Jacobs, M., Furie, B. C., and Furie, B. (1996) *J. Biol. Chem.* **271,** 16227–16236
5. Freedman, S. J., Furie, B. C., Furie, B., and Baleja, J. D. (1995) *Biochemistry* **34,** 12126–12137
6. Freedman, S. J., Furie, B. C., Furie, B., and Baleja, J. D. (1995) *J. Biol. Chem.* **270,** 7980–7987
7. Soriano-Garcia, M., Padmanabhan, K., de Vos, A. M., and Tulinsky, A. (1992) *Biochemistry* **31,** 2554–2566
8. Li, L., Darden, T. A., Freedman, S. J., Furie, B. C., Furie, B., Baleja, J. D., Smith, H., Hiskey, R. G., and Pedersen, L. G. (1997) *Biochemistry* **36,** 2132–2138
9. Shikamoto, Y., Morita, T., Fujimoto, Z., and Mizuno, H. (2003) *J. Biol. Chem.* **278,** 24090–24094
10. Banner, D. W., D'Arcy, A., Chene, C., Winkler, F. K., Guha, A., Konigsberg, W. H., Nemerson, Y., and Kirchhofer, D. (1996) *Nature* **380,** 41–46
11. Mizuno, H., Fujimoto, Z., Atoda, H., and Morita, T. (2001) *Proc. Natl. Acad. Sci. U. S. A.* **98,** 7230–7234
12. Zhou, Y., Morais-Cabral, J. H., Kaufman, A., and MacKinnon, R. (2001) *Nature* **414,** 43–48
13. Suggett, S., Kirchhofer, D., Hass, P., Lipari, T., Moran, P., Nagel, M., Judice, K., Schroeder, K., Tom, J., Lowman, H., Adams, C., Eaton, D., and Devaux, B. (2000) *Blood Coagul. Fibrinolysis* **11,** 27–42
14. Lewis, R. M., Furie, B. C., and Furie, B. (1983) *Biochemistry* **22,** 948–954
15. Borowski, M., Furie, B. C., Bauminger, S., and Furie, B. (1986) *J. Biol. Chem.* **261,** 14969–14975
16. Liebman, H. A., Furie, B. C., and Furie, B. (1987) *J. Biol. Chem.* **262,** 7605–7612
17. Refino, C. J., Himber, J., Burcklen, L., Moran, P., Peek, M., Suggett, S., Devaux, B., and Kirchhofer, D. (1999) *Thromb. Haemostasis* **82,** 1188–1195
18. Refino, C. J., Jeet, S., DeGuzman, L., Bunting, S., and Kirchhofer, D. (2002) *Arterioscler. Thromb. Vasc. Biol.* **22,** 517–522
19. Otwinowski, Z., and Minor, W. (1997) *Methods Enzymol.* **276,** 307–326
20. Navaza, J. (1994) *Acta Crystallogr. Sect. A* **50,** 157–163
21. Guex, N., and Peitsch, M. C. (1997) *Electrophoresis* **18,** 2714–2723
22. Brunger, A. T., Adams, P. D., Clore, G. M., DeLano, W. L., Gros, P., Grosse-Kunstleve, R. W., Jiang, J. S., Kuszewski, J., Nilges, M., Pannu, N. S., Read, R. J., Rice, L. M., Simonson, T., and Warren, G. L. (1998) *Acta Crystallogr. Sect. D Biol. Crystallogr.* **54,** 905–921
23. Read, R. J. (1986) *Acta Crystallogr. Sect. A* **42,** 140–149
24. Jones, T. A., Zou, J.-Y., Cowan, S. W., and Kjeldgaard, M. (1991) *Acta Crystallogr. Sect. A* **47,** 110–119
25. Kraulis, P. J. (1991) *J. Appl. Crystallogr.* **24,** 946–950
26. Esnouf, R. M. (1999) *Acta Crystallogr. Sect. D Biol. Crystallogr.* **55,** 938–940
27. Merritt, E. A., and Bacon, D. J. (1997) *Methods Enzymol.* **277,** 502–524
28. Nicholls, A., Sharp, K. A., and Honig, B. (1991) *Proteins* **11,** 281–296
29. McDonald, I. K., and Thornton, J. M. (1994) *J. Mol. Biol.* **238,** 777–793
30. Wallace, A. C., Laskowski, R. A., and Thornton, J. M. (1995) *Protein Eng.* **8,** 127–134
31. Huang, M., Syed, R., Stura, E. A., Stone, M. J., Stefanko, R. S., Ruf, W., Edgington, T. S., and Wilson, I. A. (1998) *J. Mol. Biol.* **275,** 873–894
32. Wilson, I. A., and Stanfield, R. L. (1994) *Curr. Opin. Struct. Biol.* **4,** 857–867
33. Wu, T. T., and Kabat, E. A. (1970) *J. Exp. Med.* **132,** 211–250
34. Gillis, S., Furie, B. C., Furie, B., Patel, H., Huberty, M. C., Switzer, M., Foster, W. B., Scoble, H. A., and Bond, M. D. (1997) *Protein Sci.* **6,** 185–196
35. Furie, B., and Furie, B. C. (1979) *J. Biol. Chem.* **254,** 9766–9771
36. Tai, M. M., Furie, B. C., and Furie, B. (1980) *J. Biol. Chem.* **255,** 2790–2795
37. Wojcik, E. G., Cheung, W. F., van den Berg, M., van der Linden, I. K., Stafford, D. W., and Bertina, R. M. (1998) *Biochim. Biophys. Acta* **1382,** 91–101
38. Liebman, H. A., Limentani, S. A., Furie, B. C., and Furie, B. (1985) *Proc. Natl. Acad. Sci. U. S. A.* **82,** 3879–3883
39. Sunnerhagen, M., Forsen, S., Hoffren, A. M., Drakenberg, T., Teleman, O., and Stenflo, J. (1995) *Nat. Struct. Biol.* **2,** 504–509
40. Jalbert, L. R., Chan, J. C., Christiansen, W. T., and Castellino, F. J. (1996) *Biochemistry* **35,** 7093–7099
41. Giannelli, F., Green, P. M., Sommer, S. S., Poon, M., Ludwig, M., Schwaab, R., Reitsma, P. H., Goossens, M., Yoshioka, A., Figueiredo, M. S., and Brownlee, G. G. (1998) *Nucleic Acids Res.* **26,** 265–268
42. Giannelli, F., Green, P. M., High, K. A., Sommer, S., Poon, M. C., Ludwig, M., Schwaab, R., Reitsma, P. H., Goossens, M., Yoshioka, A., and Brownlee, G. G. (1993) *Nucleic Acids Res.* **21,** 3075–3087
43. Rowley, G., Saad, S., Giannelli, F., and Green, P. M. (1995) *Genomics* **30,** 574–582
44. Gui, T., Lin, H. F., Jin, D. Y., Hoffman, M., Straight, D. L., Roberts, H. R., and Stafford, D. W. (2002) *Blood* **100,** 153–158
45. McDonald, J. F., Shah, A. M., Schwalbe, R. A., Kisiel, W., Dahlback, B., and Nelsestuen, G. L. (1997) *Biochemistry* **36,** 5120–5127
46. Park, C. H., and Tulinsky, A. (1986) *Biochemistry* **25,** 3977–3982
47. Luzzati, V. (1952) *Acta Crystallogr.* **5,** 802–810
48. Laskowski, R. A., MacArthur, M. W., Mass, D. S., and Thornton, J. M. (1993) *J. Appl. Crystallogr.* **26,** 283–291

Crystal Structure of the Calcium-stabilized Human Factor IX Gla Domain Bound to a Conformation-specific Anti-factor IX Antibody

Mingdong Huang, Barbara C. Furie and Bruce Furie

J. Biol. Chem. 2004, 279:14338-14346.
doi: 10.1074/jbc.M314011200 originally published online January 13, 2004